Power cycles integration in concentrated solar power plants with energy storage based on calcium looping

C. Ortiz [a,] *, R. Chacartegui [b], J.M. Valverde [a], A. Alovisio [c], J.A. Becerra [b]

[a] Faculty of Physics, University of Seville, Avenida Reina Mercedes s/n, 41012 Sevilla, Spain
[b] Energy Engineering Department, University of Seville, Camino de los Descubrimientos s/n, 41092 Sevilla, Spain
[c] Politecnico di Torino, Department of Energy Engineering, Corso Duca degli Abruzzi 24, 10129 Torino, Italy

* Corresponding author. Tel.: +34 655783930
E-mail address: cortiz7@us.es

Abstract

Efficient, low-cost and environmentally friendly storage of thermal energy stands as a main challenge for large scale deployment of solar energy. This work explores the integration into concentrated solar power plants of the calcium looping process based upon the reversible carbonation/calcination of calcium oxide for thermochemical energy storage. An efficient concentrated solar power-calcium looping integration would allow storing energy in the long term by calcination of calcium carbonate thus overcoming the hurdle of variable power generation from Solar. After calcination, the stored products of the reaction (calcium oxide and carbon dioxide) are brought together in a carbonator reactor whereby the high temperature exothermic reaction releases the stored energy for efficient power production when needed. This work analyses several power cycle configurations with the main goal of optimizing the performance of the overall system integration. Possible integration schemes are proposed in which power production is carried out directly (using a closed carbon dioxide Brayton power cycle) or indirectly (by means of a steam reheat Rankine cycle or a supercritical carbon dioxide Brayton cycle). The results obtained show that the highest plant efficiencies (up to 45-46%) are achievable using a closed carbon dioxide Brayton power cycle.

Keywords

Global warming, Renewable energies, Concentrated Solar Power (CSP), Thermochemical energy storage (TCES), Calcium looping (CaL), Power cycles, Supercritical CO_2 power cycle.

1. Introduction

The commercial expansion of renewable energy technologies is an urgent need to limit global warming to “well below” 2.0°C (by 2100) and pursue 1.5°C above pre-industrial levels as was at Paris COP21 Conference [1]. In particular, Concentrated Solar Power (CSP) should play a leading role within the new energy landscape as it lends itself to potentially cheap storage of energy in the form of heat [2]. Thus, efficient and affordable thermal energy storage systems must be developed in order to decouple production and demand [3], which would allow a deep penetration of solar energy power generation into the grid.

In recent years a large number of potential thermal storage technologies for medium to high temperature CSP systems have been proposed [4] based upon three main concepts: i) sensible Thermal Energy Storage (TES), such as direct steam storage [5] or molten salt systems [6,7]; ii) latent heat storage using Phase Change Materials (PCMs), on which Zalba et al. [8] published a comprehensive review of materials and applications; and iii) Thermochemical Energy Storage (TCES). Regarding to TCES, a large number of potential systems [9], experimental research under practical conditions [10] and TCES reactor designs [11] can be found in literature. Essentially, TCES consists of using the heat obtained from an external source, such as CSP, to drive an endothermic reaction. When energy is needed, the separately stored by-products of the reaction are brought together at the necessary conditions for the reverse exothermic reaction to occur, which releases the previously used heat for power production. The main advantages of TCES as compared to TES and PCMs are the considerably high energy density attainable, which is well above the energy density of molten salts currently used in commercial plants (~ 0.5 GJ/m^3) [12], and the possibility of storing energy in the long term [9]. An extended review on long-term solar heat storage can be found in ref. [13]. Moreover, in addition to the chemically stored heat, sensible heat stored in the reaction by-products is also usable.

The focus of the present manuscript is on TCES in CSP tower plants. In order to achieve an efficient and cost-effective thermochemical storage process, a proper selection of the reversible reaction is a crucial issue. Among the possibilities explored for TCES in CSP tower plants at large scale, one of the most promising systems is the Calcium Looping (CaL) process, which relies on the carbonation-calcination reaction of calcium oxide (CaO) (Eq. (1)) [14]. The use of several CaO precursors for TCES in CSP plants has been analysed in [15].

$$\mathrm{CaO}_{(s)} + \mathrm{CO}_{2(g)} \rightleftarrows \mathrm{CaCO}_{3(s)} \qquad \Delta H_r^0 = -178 \text{ kJ/mol} \tag{1}$$

Generally, the CaL process would begin with the decomposition of calcium carbonate ($CaCO_3$) particulate solids in a calcination reactor (calciner) yielding CaO and CO_2 as by-products. A high energy input is necessary to rise the solids stream temperature up to the value required for the reaction to occur at a sufficiently fast rate and to carry out the endothermic calcination reaction [16]. Thus, the optimum calcination temperature is essentially determined by the composition of the gas in the calcination environment [17]. Once the sensible heat from the calciner outlet streams (CaO and CO_2 streams) is recovered, these products are separately stored. Storage conditions and time are flexible and could be accommodated to energy demand and environmental circumstances. When needed, the CaO and CO_2 products are circulated into a carbonator reactor, where energy is recovered from the carbonation reaction.

A great benefit of the CaL process is the low price (~10$/ton), wide availability and harmlessness towards the environment of natural limestone and dolomites to be used as CaO precursor [18]. However, a usually claimed drawback of the CaL process is the marked deactivation of CaO derived from these natural minerals with the number of carbonation/calcination cycles. CaO deactivation is indeed particularly relevant when the CaL process is used for CO_2 capture [19,20] under conditions that necessary involve regeneration of CaO by high temperature (around 950°C) calcination at high CO_2 partial pressure and carbonation at low CO_2 partial pressure (~0.15 bar). Nevertheless, CaL conditions to achieve a high global efficiency for TCES and electricity generation in CSP plants are radically different to those corresponding to its application for CO_2 capture [21]. In the CSP-CaL integration, carbonation would be carried out under high CO_2 partial pressure and high temperature (around or above 850ºC) whereas calcination would be ideally performed at relatively low temperature (~700ºC) under a gas easily separable from CO_2 such as Helium [17] or superheated steam [22]. Under these conditions, CaO derived from natural limestone and dolomite may exhibit a high value of the residual conversion [21].

In addition to enhancing solar energy storage capacity, advanced high efficiency CSP-TES-power cycle integrations should be developed exploiting energy storage conditions to achieve a significant improvement of CSP plant performance. Integration of power cycles in commercial CSP tower plants with thermal storage in the form of sensible heat using molten salts is limited by a maximum temperature achievable around 550-600ºC. This limitation is mainly imposed by the degradation of molten salts at higher temperatures [6,7]. In recent years, molten alkali carbonates salts (MACs) have been investigated for energy storage. According to Frangini et al. [23], temperature stability of additives limits the applicability of oxidizing MAC salts at temperatures below 650 ºC. On the other hand, thermal radiation losses at the open focal point [24] adds a further temperature limitation in currently CSP plants. This implies that most of the commercial CSP tower plants currently under operation are based in Rankine cycle process [25,26]. Peak solar to electricity conversion efficiencies in these commercial CSP tower plants are around 25-30%, with an annual solar-to-electricity conversion efficiency lower than 20% [27]. At this regard, Liu et al. [28] presents current annual efficiencies as a function of solar technology used: 13-15% for parabolic trough, 14-18% for tower ad 9-13% for Fresnel. On the other hand, the European Academies Scientific Advisory Council [29] shows the difference of annual solar to electricity efficiencies between conceptual (around 22-28%) and industrial (around 14-18%) status.

This manuscript analyses several integration schemes to use the CaL process for TCES in CSP plants. Integration models aimed at similar goals have been already investigated by other authors. Tregambi et al. [30] proposed a scheme whereby calcination in the CaL process is assisted by CSP for CO_2 capture in a coal fired power plant. Edwards et al. [31] investigated a CSP-CaL integration in which the heat produced in the carbonator reactor is used for power generation through a CO_2/air open cycle. This configuration assumes that the CO_2 stream entering into the carbonator reacts completely with the CaO solids to produce $CaCO_3$. However, attending to the reaction equilibrium, carbonation will be ceased when the CO_2 partial pressure in the carbonator reactor reaches the equilibrium partial pressure (see Equation 8). Thus, CO_2 in the carbonator effluent gas will be unavoidably released to the environment in a CO_2/air open cycle at a concentration depending on the carbonator temperature. In order to guarantee the absence of CO_2 emissions, alternative power cycles must be employed. In this regard, Chacartegui et al. [32] have recently proposed a CSP-CaL integration wherein the TCES system is integrated with a closed CO_2 power cycle directly coupled to the carbonator following a pinch-analysis methodology [33]. In the discharge operation the circulating CO_2 passes directly to the carbonator and power turbine. The present manuscript explores the integration with the TCES core system of alternative direct and indirect cycles (steam turbine, closed Brayton CO_2 and indirect-supercritical CO_2)) for relevant CSP-CaL integration conditions. The obtained results show that the highest efficiencies are achieved using direct cycles, potentially reaching global power efficiencies above 44%.

2. CSP-CaL integration model

In this section the main aspects of the CSP-CaL integration model based on mass and energy balance in heat exchangers, solid reservoirs, CO_2 storage tank and reactors are summarized. The interested reader is referred to [32] where the model is described in detail. Moreover, the main CSP-CaL model simulation results are analysed as a previous step to discuss the power cycle integration.

2.1. Model description

Figure 1 shows a schematic representation of the CSP-CaL integration model. The process starts in the solar receiver, where solar energy input is used to carry out the calcination of $CaCO_3$ (endothermic reaction). Currently commercial CSP tower systems would allow achieving temperatures in the range of 700-900ºC, which are high enough to drive limestone calcination in short residence times [21] using a solar calciner reactor among those already proposed in the literature [34]. Thus, Meier et al. [35] have developed a solar multi-tube rotary kiln prototype for carrying out the calcination reaction at temperatures up to 1100ºC. Once calcination takes place, the released CO_2 is sent to a storage tank after being cooled and compressed whereas the CaO stream is transported to a solids reservoir. Both streams exiting the calciner at high temperature are passed through a heat exchanger network to extract their sensible heat as a previous step to storage at ambient temperature. This is a main advantage of the CSP-CaL integration over current state of the art sensible heat storage using molten salts, whose temperature must be kept above ~200°C to avoid solidification [36]. In order to use reasonably sized CO_2 storage volumes a minimum pressure of 75 bar is needed to store CO_2 storage under supercritical conditions (considering storage at ambient temperature) [32]. The high compression ratio from calciner to storage conditions (1:75) requires the use of intercooling compression to minimize the efficiency penalty. Solids transport can be carried out by means of pneumatic conveying, an already mature technology to transport high temperature granular solids [37]. For Ca based particles and a typical transport length of 200 m, an energy consumption of 20 MJ/ton has been used in the CSP-CaL integration model [32].

When power is needed the energy stored is released in the carbonator through the exothermic carbonation reaction. According to thermodynamic reaction equilibrium carbonation can be carried out at high temperature (>850ºC) under high CO_2 partial pressure [38]. This would allow a highly efficient generation of electricity thus overcoming temperature limits (T~550-600°C) in currently commercial CSP plants with thermal storage in molten salts. Solids exiting the carbonator are passed through another heat exchanger network to preheat the CaO and CO_2 streams entering the carbonator. After the storage step, the CO_2 stream is expanded to the selected carbonator pressure, which must be below the storage pressure in order to use the commercial fluidized bed technology. As can be seen in Figure 1, compression-expansion process of CO_2 before and after the storage step resembles a compressed air energy storage (CAES) system [4]. Thus, besides of sensible and thermochemical energy storage, the integration compresses orates energy storage also in the form of compressed gas with a round trip efficiency of about 67% using a compression-expansion train (see [32] for further details).

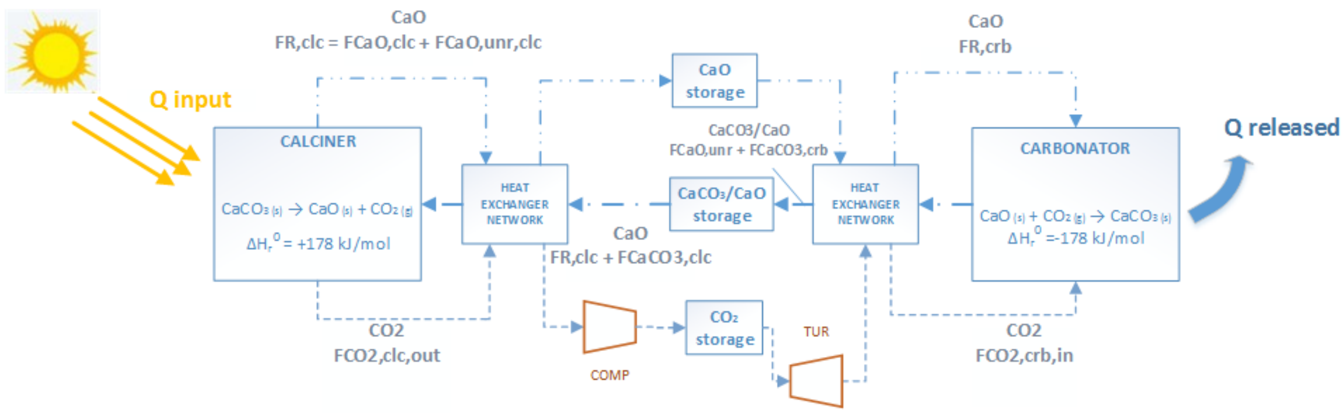

Figure 1: CSP-CaL integration scheme

As can be seen in Figure 1, only a fraction of the total flow rate of CaO entering into the carbonator ($F_{R,crb}$) reacts with CO_2 to produce $CaCO_3$ ($F_{CaCO3,crb}$), remaining the rest as unreacted CaO ($F_{CaO,unr}$). The average CaO conversion (or activity) X determines the amount of CaO converted to $CaCO_3$ in the carbonator ($X = F_{CaCO3,crb}/F_{R,crb}$). On the other hand, the carbonated particles entering into the calciner reactor are assumed to achieve a complete decomposition, yielding one mole of CO_2 ($F_{CO_2,clc,out}$) and one mole of regenerated CaO ($F_{CaO,clc}$) for each mole of $CaCO_3$ ($F_{CaCO_3,clc}$) according to equation (1).

The streams circulating in either the calciner or carbonator sides are decoupled. Thus, the solar calciner only works in the daytime and under clear sky conditions whereas the carbonator reactor must operate on demand during a 24h period, which requires a properly storage vessel sizing. More sophisticated control strategies should be devised within a framework of long-period control to ensure steady operation over time lags beyond 24h. Such control should rely on meteorological forecasts and the power load curve. Thus, in order to guarantee a steady-state operation, the mass-balance equation:

$$\int_{24h} F_{CaCO3,clc}(t)\,dt = \int_{24h} F_{CaCO3,crb}(t)\,dt \tag{2}$$

must be satisfied. An average daytime period (Δt_{sun}) is assumed during which solar irradiation is sufficiently intense to attain full calcination. In this case Equation (2) can be derived to obtain:

$$\overline{F_{CaCO_3,clc}} \cdot \Delta t_{sun} = \overline{F_{CaCO_3,crb}} \cdot 24 \tag{3}$$

For energy balance, the first thermodynamics law is applied to the carbonator and calciner reactors:

$$\sum_i F_{i,out} h_{i,out} - \sum_i F_{i,in} h_{i,in} = \Phi - \dot{W} \tag{4}$$

$$F_{i,out} - F_{i,in} = \xi \nu_i \tag{5}$$

where ξ denotes the extent of reaction per unit time. Arranging and considering that output conditions are reactor conditions, it is:

$$\xi \Delta H_R(T_{react}) + \sum_i F_{i,in}\,(h_{i,react} - h_{i,in}) = \Phi - \dot{W} \tag{6}$$

with

$$\Delta H_R(T_{react}) = \sum_i \nu_i h_{i,T} = \Delta H_R^0 + \sum_i \nu_i \int_{ref}^{T_{react}} c_{p,i}\,dT \tag{7}$$

being the reaction enthalpy change at the reaction temperature.

2.2. Model results

The proposed CSP-CaL integration model has been simulated to assess the integration efficiency. A sensitivity analysis has been carried out on relevant CaL cycle parameters such as CaO average conversion X and carbonation equilibrium conditions [39]. Data used for the reference case are reported in Table 1.

Table 1: CSP-CaL reference case simulation data

Net absorbed solar heat flux in calciner	100	MWt
Thermal dispersions in carbonator	10	%
Calciner temperature	900	°C
Calciner pressure	1	bar
Ambient temperature	20	°C
CaO average conversion (X)	0.5	
Carbonator temperature	875	°C
Carbonator pressure	7	bar
CO_2 storage conditions	75	bar, T ambient
Solid phase conveying energy consumption	20	MJ/ton
Daylight hours (constant solar flux)	8h	
Isentropic efficiencies (compression/expansion)	0.89	

CaO average conversion has a significant influence on the solids flow rates, storage vessels, power production and consumption, and heat exchangers network configuration. Thus, a high CaO conversion leads to a low fraction of unreacted CaO left, which affects relevantly the plant's performance. As the average CaO conversion increases the solids mass flow rate is decreased (Figure 2), therefore energy consumption due to solids conveying is reduced.

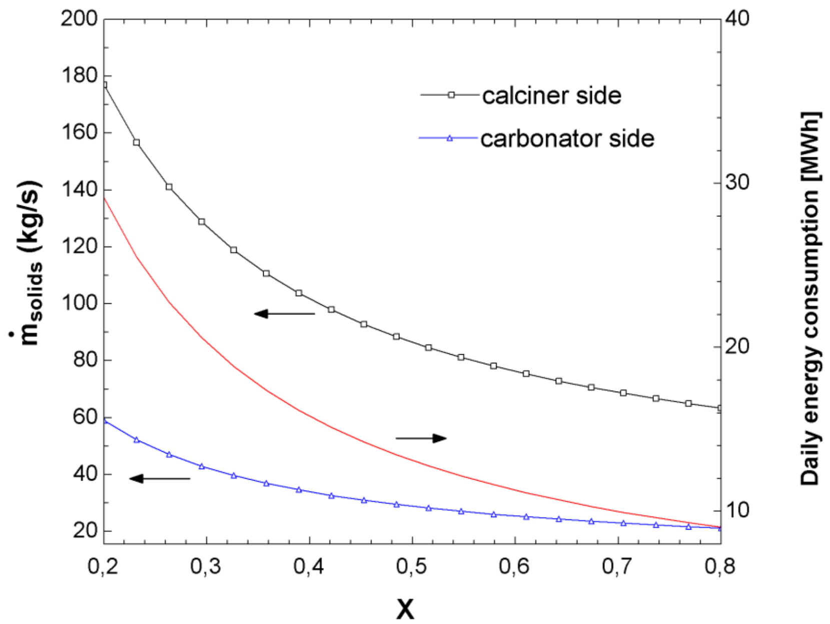

Figure 2: Solids mass flow rate (left axis) and daily energy consumption (right axis) due to solids conveying as a function of average CaO conversion (X)

Figure 3 shows the effect of the average CaO conversion on the thermal power effectively used for energy storage. Keeping fixed a 100 MW_{th} of CSP input (ϕ_{CSP}) into the system, the thermal power used to carry out the calcination reaction ($\phi_{calcination}$ = 92 MWth) does not depend on the solids conversion in the carbonator while the rest (8 MWth) is employed to raise the solids temperature before entering into the calciner. A part of the released power in the carbonator $\phi_{released,crb}$ is used to increase the temperature of the inlet streams up to the carbonation temperature, which leaves the rest of thermal energy available $\phi_{available}$ to be used in the power cycle for electricity production. The difference between calcination and carbonation power is due to thermal energy dispersions in the carbonator (10%).

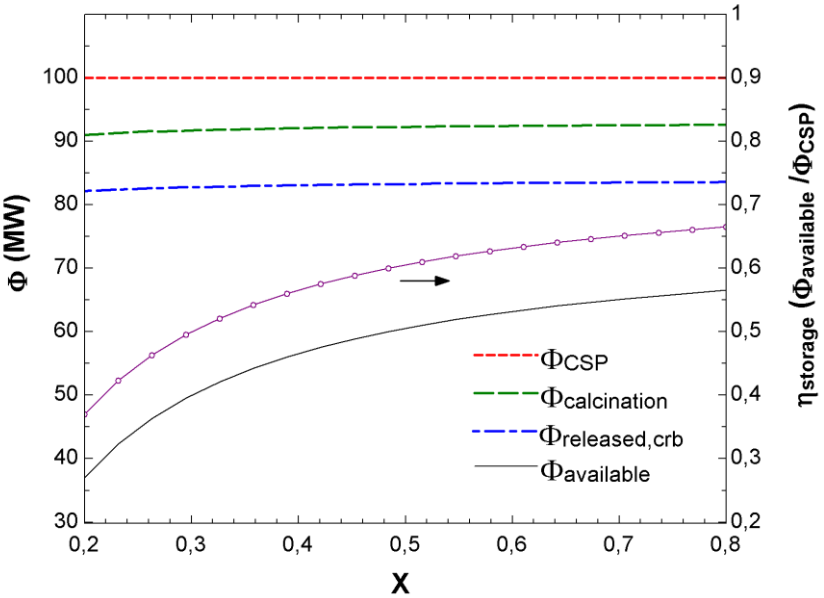

Figure 3: Thermal power fluxes (left axis) and energy storage efficiency (right axis) as a function of average CaO conversion in the carbonator.

Another relevant issue to be considered is that increasing the average CaO conversion allows for an important reduction of the solids storage volumes as can be seen in Figure 4a. On the other hand, a change in *X* does not yield a significant variation of the CO_2 storage volume, which is however quite sensitive to CO_2 density as determined by storage pressure and temperature (Figure 4b).

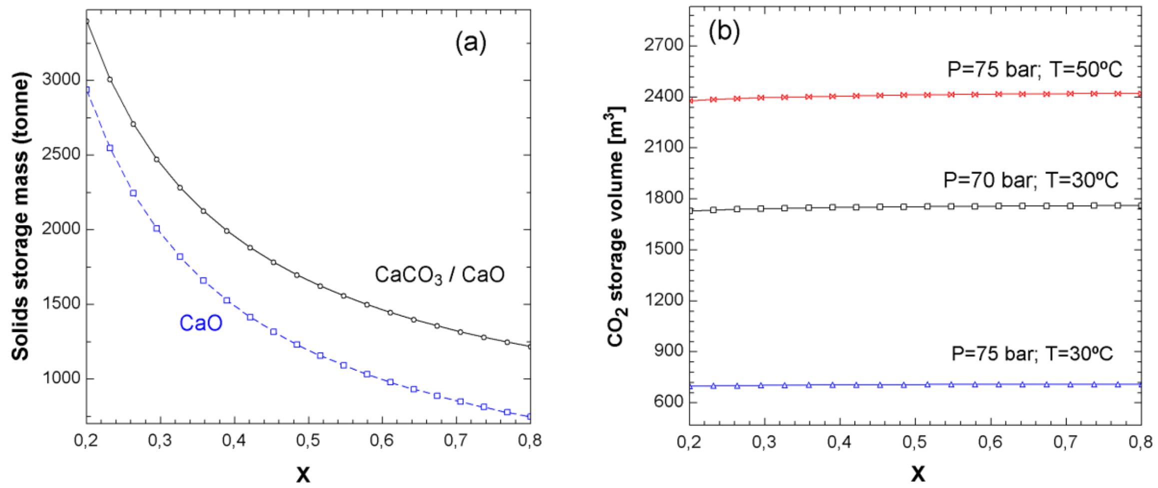

Figure 4: (a) Solids storage mass as a function of average CaO conversion. (b) CO_2 storage volume as a function of average CaO conversion for several storage conditions.

Previous works on the CaO multicycle conversion in the CaL process have been mostly focused on Post-Combustion CO_2 Capture (PCCC) conditions, either on laboratory-physical analysis [20,40], reactor modelling [41] or process integration models [42], involving in all cases carbonation under relatively low CO_2 partial pressure (~ 0.15 bar) and calcination at very high temperatures (~ 950ºC) under high CO_2 partial pressure. Under these conditions the CO_2 sorbent (CaO) presents a severe drop of conversion after a few cycles converging towards a residual value of just about 0.07-0.08 [43,44]. Nevertheless, it is important to remark that the CSP-CaL integration for thermochemical energy storage involves CaL conditions radically diverse from those in the case of PCCC. Thus, thermogravimetric analysis (TGA) tests show that the residual conversion of limestone derived CaO can be as large as X_r=0.5 for conditions that correspond to the optimum CSP-CaL integration that involve carbonation at high temperature under high CO_2 partial pressure [21]. Moreover, according to TGA results fast calcination may be achieved at a reduced temperature of just 700-725ºC under a gas which is easily separable from CO_2 (either He as in the TGA experiments described in [21] or superheated steam [22]). Attaining such a low calcination temperature would allow the use of already mature and inexpensive metallic solar receivers thus reducing technological risks. On the other hand, the work of He/CO_2 or H_2O/CO_2 separation should be also included in an extended techno-economic energy analysis.

Carbonator conditions (pressure and temperature) are highly relevant for the global CSP-CaL power cycle integration. Carbonator pressure is selected by considering the most favorable conditions for the CaL-power cycle integration, i.e. a fluidized bed reactor operated under atmospheric pressure if an indirect power cycle is integrated and a pressurized fluidized bed reactor for direct integration with a power cycle, in order to achieve the higher integration performance. On the other hand, increasing the carbonator temperature (T_{carb}) leads to higher power cycle efficiencies and therefore enhances the CSP-CaL-power cycle integration performance. However, the maximum temperature in the carbonator is limited by the thermodynamic equilibrium of the carbonation/calcination reaction. Thus, for a given CO_2 partial pressure in the carbonator there is a maximum carbonator temperature above which the carbonation reaction is not thermodynamically favourable. According to thermochemical data [38], the CO_2 partial pressure for the reaction to be at equilibrium at a given temperature T(K) is given by:

$$P_{eq}(bar) = P \cdot y_{eq} = \left[4.137\ 10^7 \exp\left(-\frac{20474}{T}\right)\right] \tag{8}$$

In Eq. (8), y_{eq} is the fraction of CO_2 in the carbonation environment. For a fixed carbonator temperature, there is a minimum carbonator pressure below which the CO_2 partial pressure is insufficient for carbonation to occur. Figure 5 shows the minimum carbonator pressure as a function of reactor temperature to carry out carbonation and for different CO_2 fractions (equation (8)). It is clear that operating under pure CO_2 $(y_{CO2,in} = 1)$ allows working under higher temperatures and low carbonator total pressures.

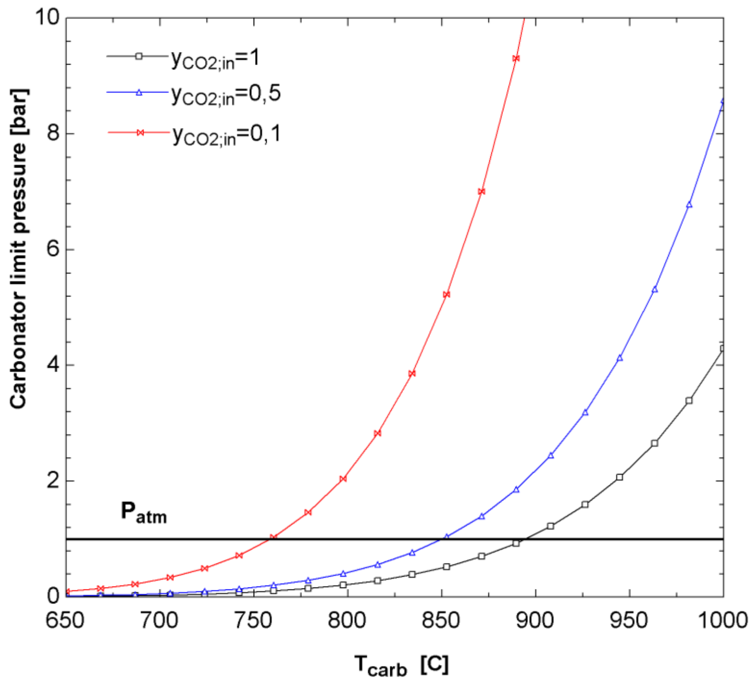

Figure 5: Minimum carbonator pressure as a function of carbonator temperature T_{carb} for several CO_2 volume concentrations at the carbonator inlet ($y_{CO2,in}$)

3. CSP-CaL-power cycle integration

This section is devoted to the study of several power cycle integrations into the CaL based CSP storage system. Power cycles are classified in two categories: power cycles with direct integration (CO_2 regenerative Brayton cycle) and power cycles with indirect integration (Rankine Reheat cycle and supercritical CO_2 recompression cycle).

3.1. Direct integration

In power cycles with direct integration the heat transfer fluid used in the carbonator is sent directly into a gas turbine. In the following a CO_2 closed Brayton cycle is analysed.

a CO_2 closed Brayton cycle

In this integration scheme (Figure 6), the heat released by the carbonation reaction is delivered to a gas turbine by the excess CO_2 that does not participate in the reaction and is used as carrier through a Joule-Brayton cycle. This is therefore a direct integration between the heat released and power cycle, which has been recently studied in [32].

Figure 6 shows the CO_2 closed Brayton cycle scheme. The CO_2 power cycle is a closed and regenerative cycle, whereby the heat removed by the reactants in the carbonator is recovered in an open cyclone exchanger (HXF in Figure 6). Thus, in this heat exchanger (HXF) heat from the exhaust CO_2 stream serves to heat up the CaO solids before entering the carbonator while in HXE the residual heat from the solids at the carbonator output is extracted to pre-heat the CO_2 stream at the carbonator inlet. Part of the power needed in the compression stage of the Joule-Brayton cycle is provided by the expansion of the pressurized CO_2 used for reaction in the carbonator. In the CO_2 closed configuration the carbonator operates under a 100% CO_2 environment. Therefore, the molar flow rate of CO_2 flowing into the carbonator is by large in excess over the stoichiometric need. The CO_2 stream in the carbonator side is balanced out to use the non-reacting excess CO_2 to deliver heat of the carbonation reaction to the gas turbine for power production. Main data set used in the simulations is shown in Figure 6 as well as results obtained.

The CO_2 closed Brayton cycle presents the following characteristics:

- Regarding to chemical equilibrium considerations, by operating in a pure CO_2 atmosphere, the minimum carbonator pressure coincides with the CO_2 partial pressure, making it possible to attain carbonation temperatures of around 950°C for carbonator absolute pressures above 2.2 bar and until around 890°C for carbonator pressures above atmospheric pressure (Figure 5).
- CO_2 is characterized by lower values of both compression and expansion work compared to air.
- The CO_2 Brayton cycle provides a higher useful to expansion work ratio than an air Brayton cycle. Therefore, for a given useful work produced, the CO_2 at turbine output presents a higher enthalpy. This is beneficial from the point of view of thermal energy recovery to preheat streams entering into the carbonator (Figure 6), which enhances the plant efficiency.
- Regarding to isentropic efficiency of compressor and turbine, CO_2 is less sensitive than air, especially at the compressor [45].

Being a closed cycle, a more flexible operation is possible as compared to open cycles since possible CO_2 emissions to the atmosphere are avoided. Thus, the closed Brayton cycle could use a mix of several components as carrier fluid.

Net absorbed solar flux in calciner	100	MW
Thermal dispersions in carbonator	10	%
Ambient temperature	20	°C
CaO conversion	0.5	
Approach temperature solid-solid HX	20	°C
Approach temperature solid-gas HX	15	°C
Approach temperature CO_2 cooler	10	°C
Intercoolings in CO_2 storage compression	5	
Interheatings in CO_2 power cycle compression	8	
Interheatings in CO_2 expansion from storage	7	
Solid phase conveying energy consumption	20	MJ/tonne
Daylight hours (constant solar flux)	8h	
Isentropic efficiencies (compression/expansion)	0.89	

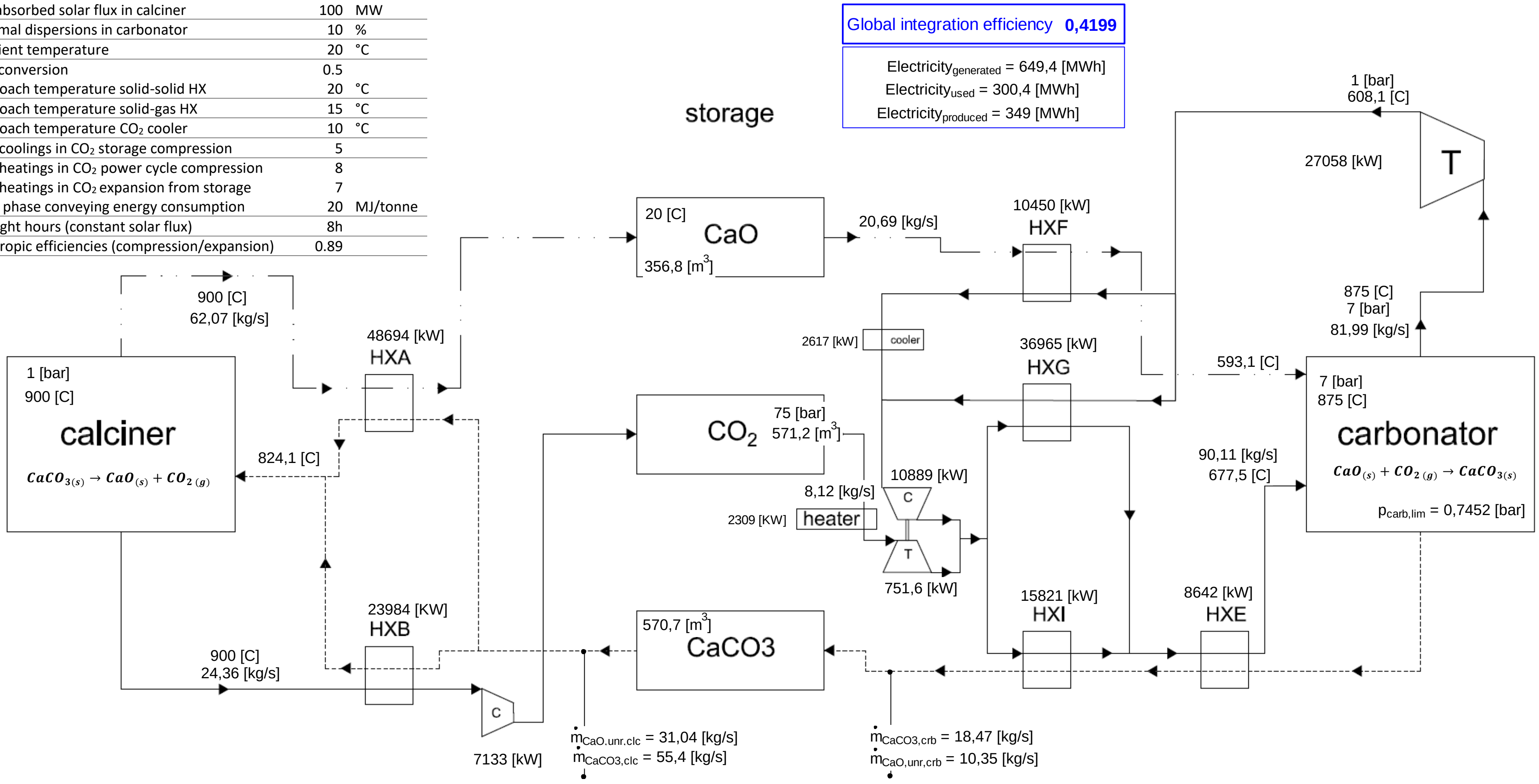

Figure 6: CSP-CaL- CO_2 closed Brayton integration scheme

A sensitivity analysis has been carried out in order to assess the global cycle performance under several Brayton cycle conditions. The cycle behaviour is analysed as affected by the pressure ratio (PR) value. PR is defined as the ratio between pressure at turbine inlet to pressure at outlet, which in this integration is given by the ratio of the carbonator pressure to the turbine outlet pressure. Figure 7 shows the relationship between PR and the carbonator inlet stream (CaO and CO_2) temperatures by keeping a fixed value of the carbonator pressure at 7 bar. As PR is increased, the turbine outlet temperature is decreased (lower value of enthalpy), which implies a lower heating capacity on the carbonator inlet streams (by means of the heat exchangers HXG, HXI and HXE in Figure 6) and therefore more carbonation heat must be used to bring the CaO and CO_2 streams to the carbonation temperature. Thus, on one hand, a high value of PR yields a higher power production in the Brayton turbine, which increases the global cycle performance. On the other, it reduces the heat available for power production, which implies a lower CO_2 mass flow rate entering into the carbonator as heat transfer fluid (left side of Figure 6). The effect of increasing PR and temperature on the global plant efficiency is shown in Figure 8. As can be seen, an increase of the carbonator temperature leads always to a higher global efficiency whereas efficiency at a given temperature has a maximum at a given value of PR.

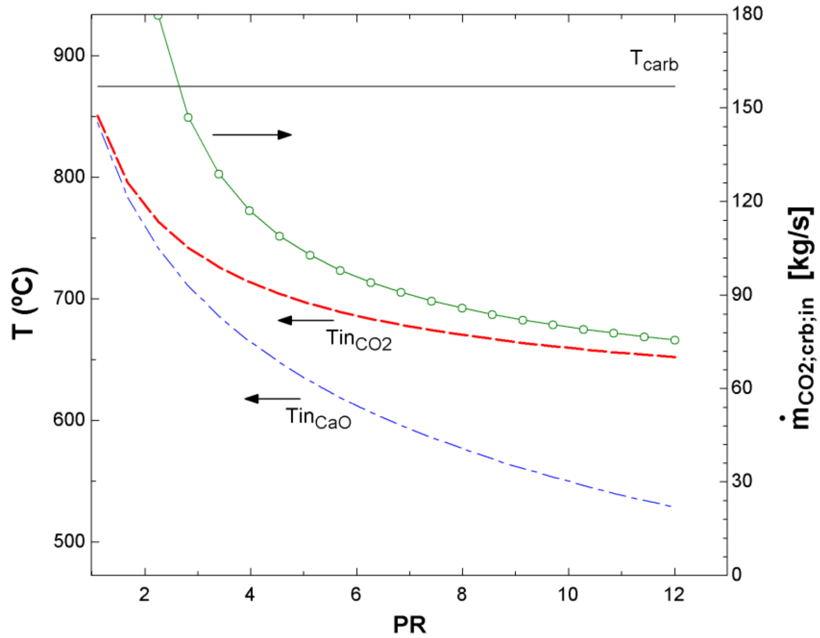

Figure 7: Left axis: Temperature of CaO (Tin_{CaO}) and CO_2 (Tin_{CO2}) streams entering into the carbonator reactor as a function of Pressure Ratio (PR). Right axis: CO_2 mass flow rate entering into the carbonator. The carbonator temperature (T_{carb}) is fixed to 875ºC

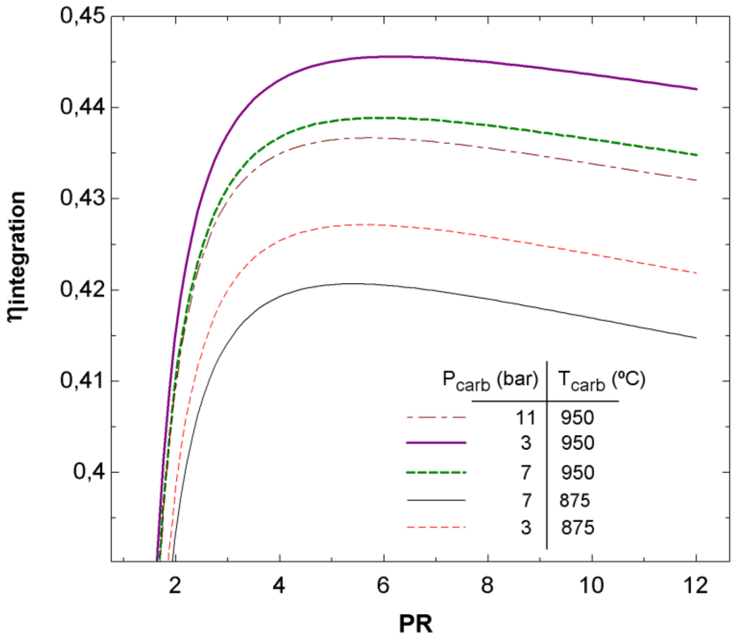

Figure 8: Global integration efficiency (CO_2 closed Brayton cycle) as a function of pressure ratio for several carbonator operation points as indicated.

3.2. Indirect integration

Regarding to indirect power cycle integration, the heat from the carbonator is transferred to the power cycle through a heat exchanger network. In this section a Rankine Reheat cycle and a supercritical CO_2 recompression cycle are analysed. Moreover, a special case based on a combined cycle is investigated.

a Reheat Rankine cycle

Currently commercial CSP tower plants incorporate the steam Rankine power cycle technology for power production [28]. As a previous step to integration within the CSP-CaL cycle, a simple reheat Rankine cycle has been modelled to analyse the power cycle efficiency. Figure 9 shows a schematic of the cycle model, which is based on a reheat Rankine cycle with regeneration from five feed-water heaters (HE1:4), one of which is a total mixer exchanger type (DEA). For this reason, a series of steam extractions (Figure 9) are realized. The steam operational parameters and benchmarking have been chosen from data of similar real power plants [46,47]. Turbine and pump efficiencies values of 0.9 have been considered, as well as heat exchangers minimum temperature difference of 10ºC. On the other hand, a 1% pressure drop is assumed in all heat exchangers. Tables 2 and 3 show the main simulation results obtained for the system schematized in Figure 9.

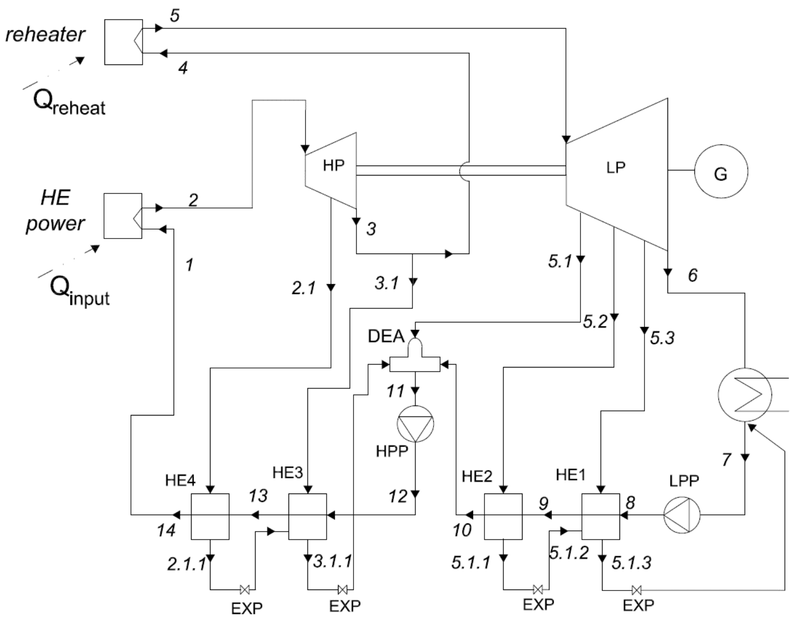

Figure 9: Base reheat Rankine cycle layout

Table 2: Main simulation Rankine cycle results for a 50MWth steam power cycle (P_{vv} = 160 bar, T_{vv} = 540/540ºC)

Q_{input}	50 MW_{th}
Q_{reheat}	9.1 MW_{th}
$W_{pump,HPP}$	0.35 MW_e
$W_{pump,LPP}$	0.03 MW_e
$W_{turb,HP}$	6.99 MW_e
$W_{turb,LP}$	18.82 MW_e
P_{HE1}	5.46 MW_{th}
P_{HE2}	2.68 MW_{th}
P_{HE3}	8.64 MW_{th}
P_{HE4}	3.88MW_{th}
η_{cycle}	43.07 %

Table 3: Stream data for a 50MWth steam power cycle (P_{vv} = 160 bar, T_{vv} = 540/540ºC)

$Stream$	$\dot{m}(kg/s)$	T (ºC)	P (bar)	$Stream$	$\dot{m}(kg/s)$	T (ºC)	P (bar)
1	22.67	315.9	204	5.2.1	1.16	132	4.95
2	22.67	540	200	5.3	1.08	99.63	1
2.1	2.45	452.1	93	5.3.1	2.23	58.6	0.99
2.1.1	2.45	294.8	92.1	6	14.29	43.77	0.09
3	20.18	352	46	7	16.53	43.58	0.09
3.1	2.02	352	46	8	16.53	43.59	18.4
3.1.1	4.51	215	45.5	9	16.53	122	18.2
4	18.16	352	46	10	16.53	159.8	18
5	18.16	540	45.5	11	22.67	202.9	18
5.1	1.63	403.7	18	12	22.67	205	208
5.2	1.16	248.5	5	13	22.67	284.8	205.9

Once the power cycle block model is developed, this is integrated into the CSP-CaL scheme. CSP-CaL main operation parameters are the same as in previous schemes (Figure 6). Pure CO_2 is used for carbonation, which allows operating at high carbonator temperatures.

Figure 10 shows a schematic representation of the CSP-CaL-Rankine integration and main simulation results considering carbonation at 875ºC under atmospheric pressure. The integration efficiency is shown in Figure 11 as a function of the carbonator pressure for diverse temperatures. As can be seen, the maximum efficiency (around 35.5%) is obtained at 875ºC operating under atmospheric pressure, which is well over current CSP plant performances. Higher temperatures in the carbonator would require higher minimum carbonator pressures for carbonation to be thermodynamically favourable at which efficiency is decreased.

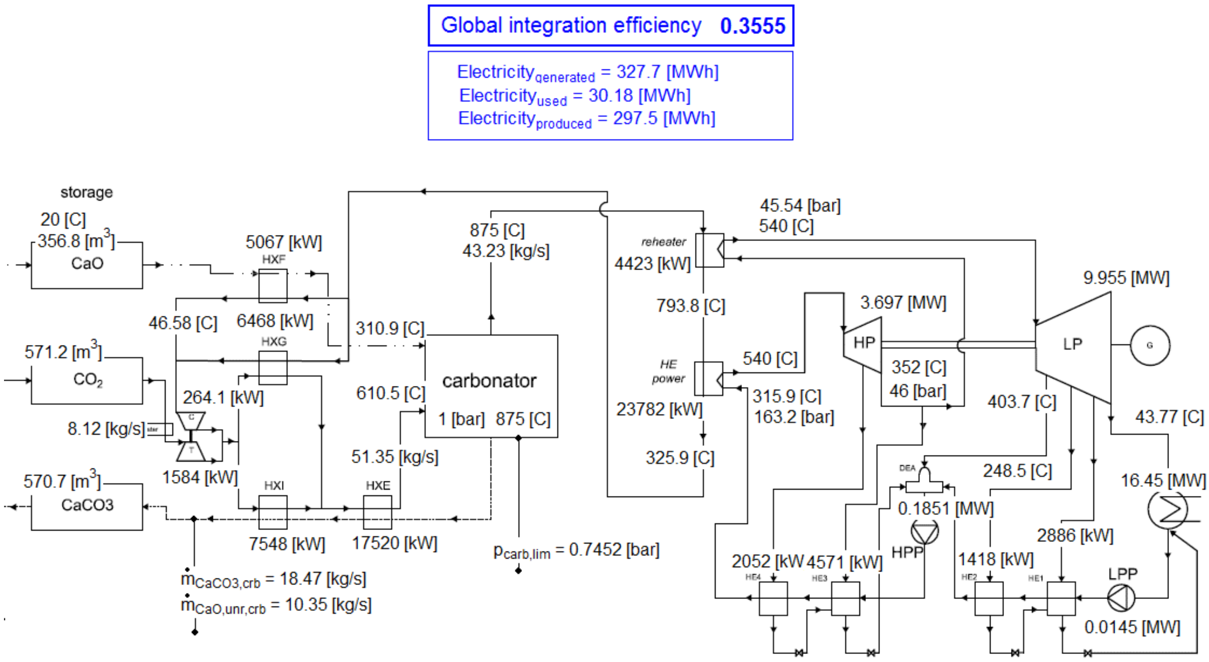

Figure 10: CSP-CaL- Regenerative Rankine integration scheme and main simulation results for carbonation under 1 bar at 875ºC.

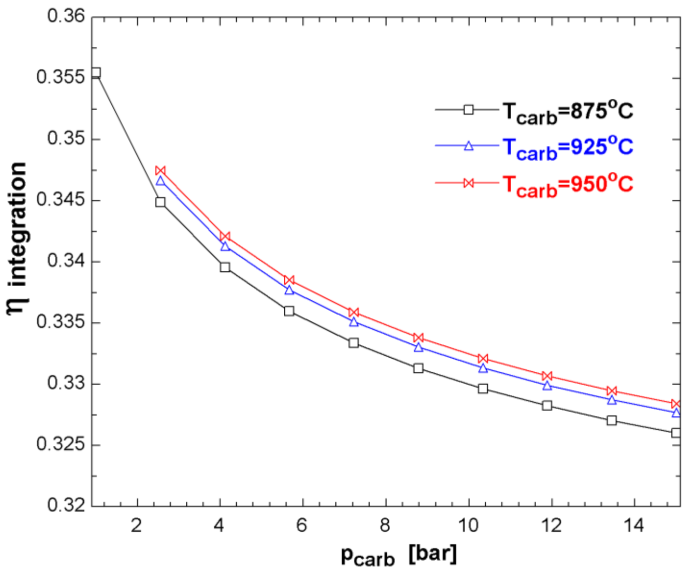

Figure 11: Efficiency of the CaL-Rankine integration as a function of carbonator pressure and for diverse temperatures. Note that a minimum carbonator pressure is required according to thermochemical equilibrium as temperature is increased.

A sensitivity analysis has been carried out in which the main Rankine cycle parameters have been tuned. As can be seen in Figure 12, the global integration efficiency is promoted by increasing live steam conditions (pressure (P_{vv}) and temperature (T_{vv})). It may be also seen that efficiency is enhanced as the reheat temperature is increase.

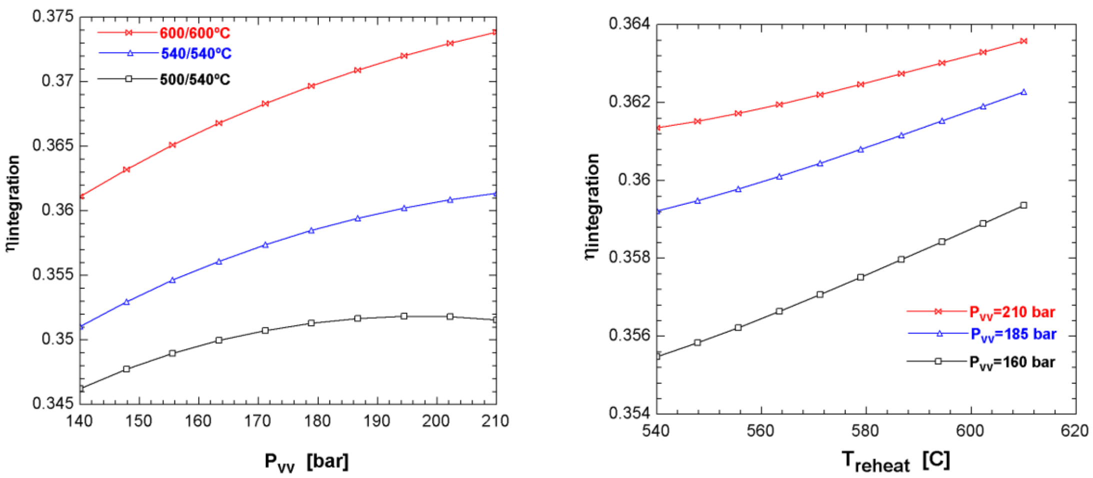

Figure 12: Global integration efficiency as a function of (LEFT) steam turbine inlet and (RIGHT) reheat temperature conditions

As seen in Figure 10, the preheat water of the Rankine cycle is heated by the exhaust CO_2 stream from the carbonator in a heat recovery steam generator (HRSG) until super-heated status is reached. One key parameters in Rankine power cycles is the HRSG efficiency, which can be analysed from the pinch point value across the steam production process. Figure 13 shows that lower values of the pinch point (higher HRSG efficiency) causes an increase in the global cycle efficiency.

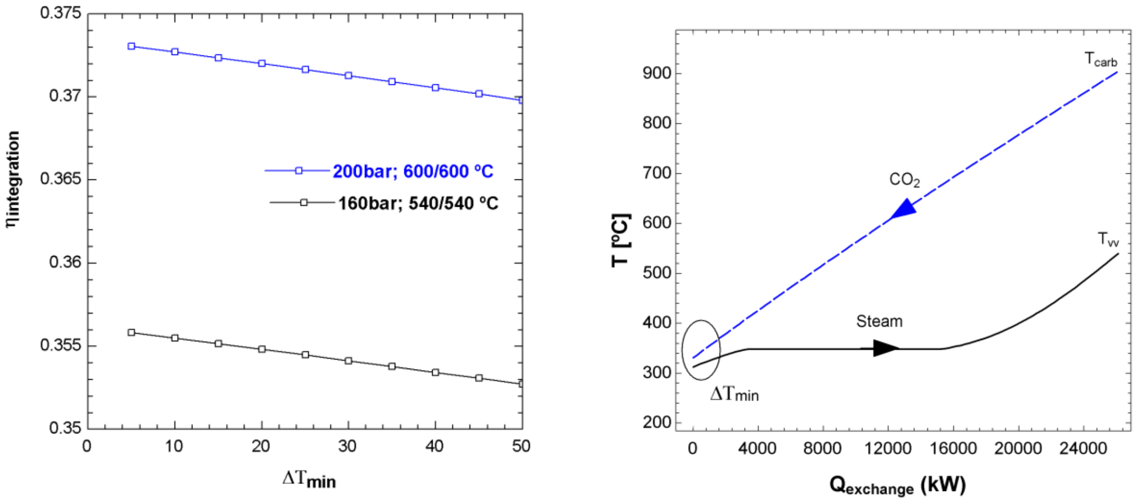

Figure 13: Global integration efficiency as a function of minimum temperature approach in HRSG

b Supercritical CO_2 (sCO_2) recompression cycle

The supercritical CO_2 (sCO_2) Brayton cycle, which was originally introduced by Feher [48], has emerged in the last years as a promising technique for high-efficiency power production. It basically consists of a closed-loop Brayton cycle that operates entirely above CO_2 critical pressure (73.77 bar and 30.98ºC) and presents a high drop in compressibility, which brings about a similar reduction in compression work while the turbine operates with CO_2 in a close to ideal behaviour. Among different layouts proposed for sCO_2 cycles, a recompression scheme seems to be the highest efficiency cycle [49], which is thus the one used in the present study. Figure 14 shows the recompression cycle model. An important feature of the regeneration process in the sCO_2 Brayton cycle is that the specific heat of the cold side is 2-3 times higher than the hot side. Thus, the CO_2 stream is split (stream 5b in Figure 14a) to compensate for the specific heat difference in the low temperature recuperator, which maximizes the heat recuperation.

CSP-sCO_2 integration models have been already developed to increase the CSP power plant performance. Thus, Chacartegui et al. [50] compared the integration of supercritical and transcritical carbon dioxide cycles as well as a combined cycle composed by a topping Brayton CO2 cycle and a bottoming Organic Rankine Cycle. Iverson et al. [51] presents the behaviour of Brayton cycle turbomachinery including a data set for stable supercritical CO2 Brayton cycle operation. Moreover, Ma et al. [52] analyses the integration of sCO2 power cycles by considering sensible heat storage (thermocline system). One of the most important advantages of the sCO_2 Brayton cycle is its compact turbomachinery, albeit it is still under development [53]. A sCO_2 technology review is presented in [45], from which values on turbomachinery efficiency and pressure drops are taken in the present work. Thus, the recompression sCO_2 cycle has been simulated using data specified in table 3.

Table 4: Input data parameters for the sCO_2 cycle [45]

η_c (%)	85
η_t (%)	90
ε_{rec} (%)	95
$\Delta P_{R,hot}$ (%)	0.5

$\Delta P_{R,cold}$ (%)	1.5
$\Delta P_{R,HE}$ (%)	0.5

Figure 14a shows the recompression sCO_2 Brayton scheme proposed. Thermodynamic parameters of the streams involved in the cycle are shown in Figure 14b in a temperature (T)-entropy (S) diagram. Main sCO2 cycle simulation results are shown in Tables 5 and 6. A cycle efficiency of around 41% is obtained from this configuration, which is in agreement with results from previous works [45,54].

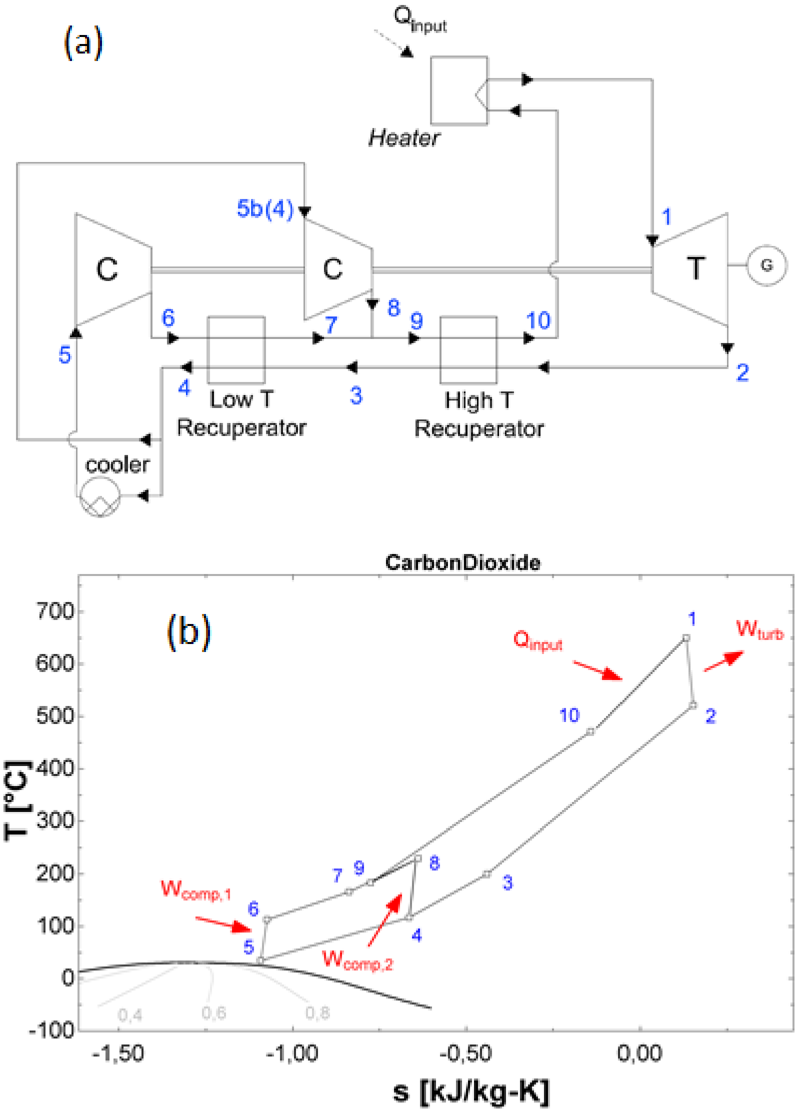

Figure 14: (a) Base recompression- sCO_2 Brayton cycle layout. (b) Temperature-entropy diagram

Once the recompression sCO_2 cycle is analysed and benchmarked it is integrated in the CSP-CaL configuration as shown in Figure 15. A global integration efficiency close to 32% is achieved, although it must be taken into account that a large amount of energy linked to the cooling process before the compression stage is not used. This suggests that a bottoming cycle could serve to improve the cycle performance [50].

Table 5: Main sCO_2 cycle simulation results

Q_{input}	50 MW_{th}
$W_{comp,1}$	7.14 MW_e
$W_{comp,2}$	5.74 MW_e
W_{turb}	33.38 MW_e
η_{cycle}	41.01 %
ϕ_{cycle}	69%

Table 6: Stream data for sCO_2 recompression cycle

$Stream$	$\dot{m}(kg/s)$	T (ºC)	P (bar)
1	223.6	650	213.9
2	223.6	521.1	78
3	223.6	200.2	77.61
4	223.6	117.2	77.22
5	158.8	35	75
5b	64.85	117.2	77.22
6	158.8	113.1	225
7	158.8	166.0	223.9
8	64.85	229.8	221.6
9	223.6	183.1	221.6
10	223.6	471	218.3

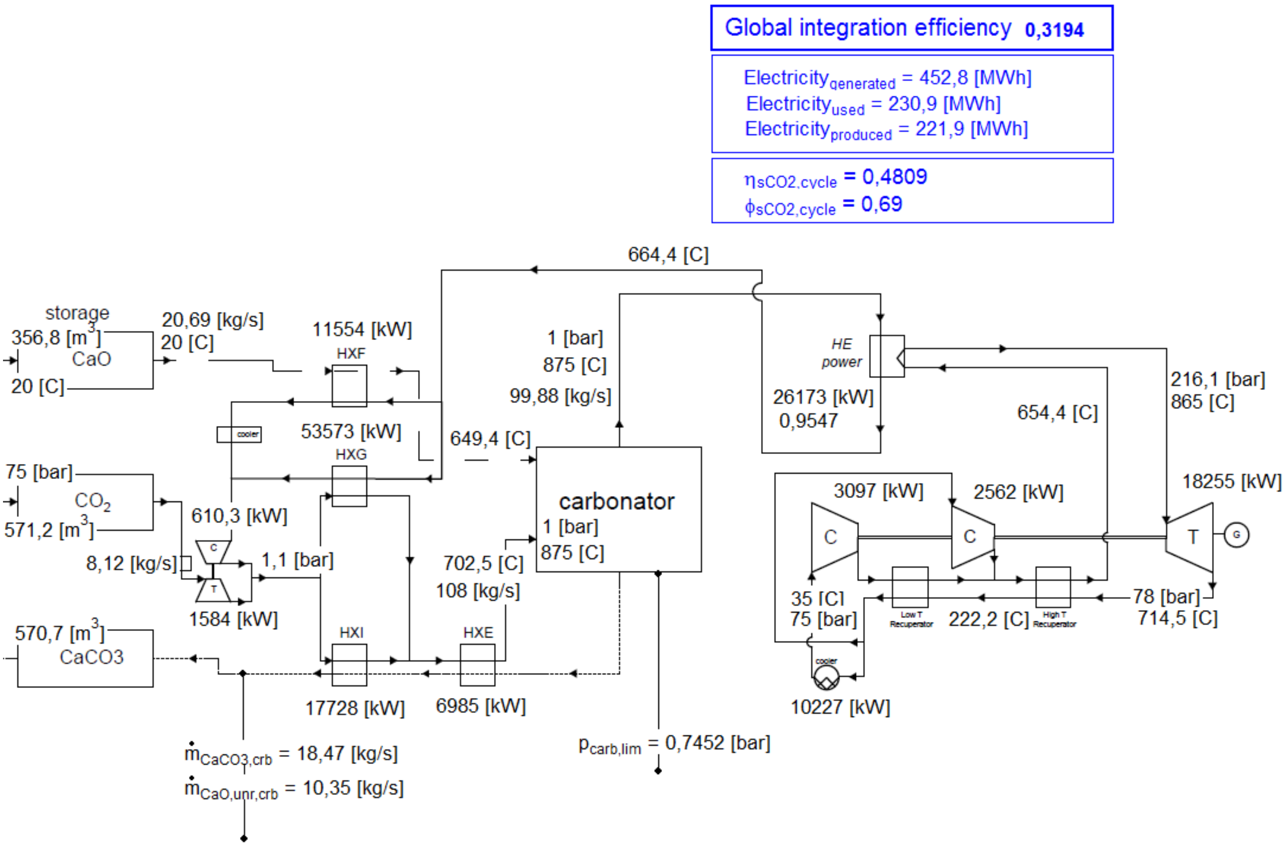

Figure 15: CSP-CaL- sCO_2 integration scheme and main simulation results

Results from a sensitivity analysis are shown in Figure 16. It is observed that the recuperation process in the sCO_2 Brayton cycle greatly influences the thermal efficiency since CO_2 properties are very sensitive to pressure and temperature near the critical point. Therefore, the hot and cold sides in the regenerator are strongly unbalanced. As can be seen in Figure 16, by increasing the turbomachinery efficiency (which depends upon further technology development) the global cycle performance is significantly enhanced.

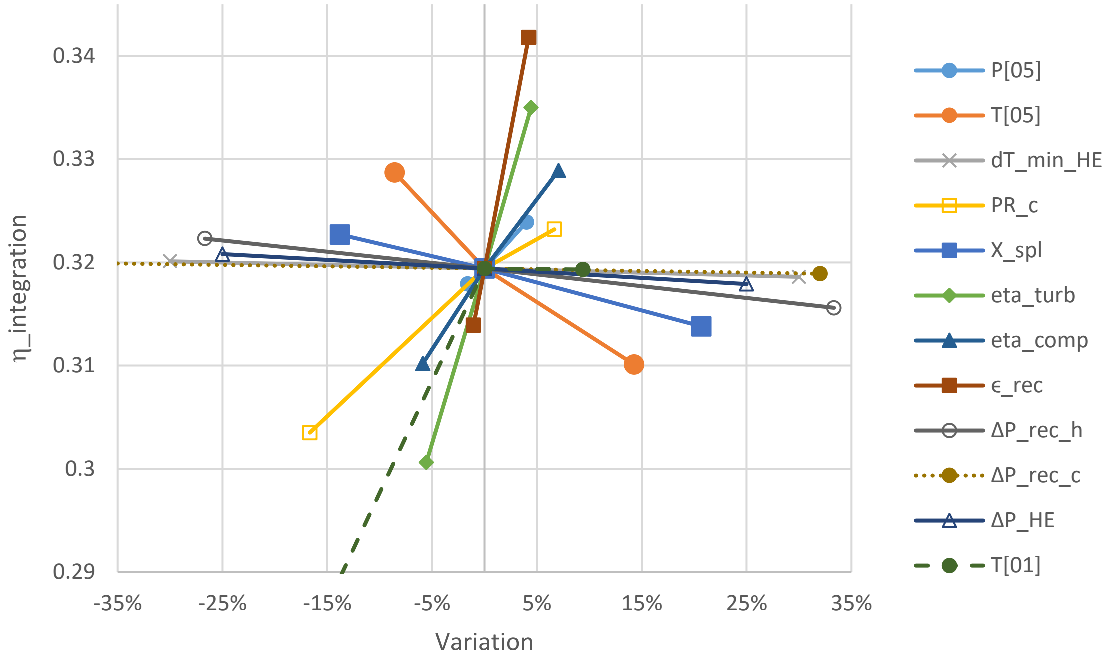

Figure 16: Sensitivity analysis results of the CSP-CaL- sCO_2 integration.

c Combined cycle

The combined cycle is based on the integration of two subsystems consisting of a gas turbine (Brayton cycle) and a steam turbine (Rankine cycle), which leads to an improvement of efficiency due to the synergy of both cycles [55].

A number of integrated solar combined cycle (ISCC) systems have been proposed to improve the power plant efficiency [56,57]. ISCCS power plants currently in operation employ the parabolic trough concentrator technology. Further work is still needed to advance in the technological readiness of solar tower – ISCC power plants [58]. ISCC cycles operate using a solar-fuel combination [59,60], with the gas turbine being fuelled by a non-solar source (based on fossil or renewable fuel) due to the temperature limitation in CSP power plants imposed by degradation of molten salts and thermal radiation losses at the focal point. Solar power share in ISCC power plants is on average below 34% [58]. Compared with the solar-only power plants, ISCC plants exhibit several advantages such as higher solar-to-electricity conversion performance. Moreover, thermal inefficiency associated with the daily start-up and shutdown of the steam turbine can be avoided [61]. Another configuration proposed in a recent work [62] evaluates a combined cycle based on a closed Brayton and organic Rankine cycle for solar power tower plants by means of energy and exergy analysis, showing that higher performance than using steam and supercritical CO_2 cycles can be achieved.

Figure 17 shows the global cycle integration proposed by considering a combined cycle for power production. The combined cycle involves a hybrid direct-indirect power cycle integration with the CSP-CaL system. The CO_2 stream exiting the carbonator is expanded in a gas turbine as a previous step for transferring heat to steam cycle through a HRSG. Main simulation results are shown also in Figure 17.

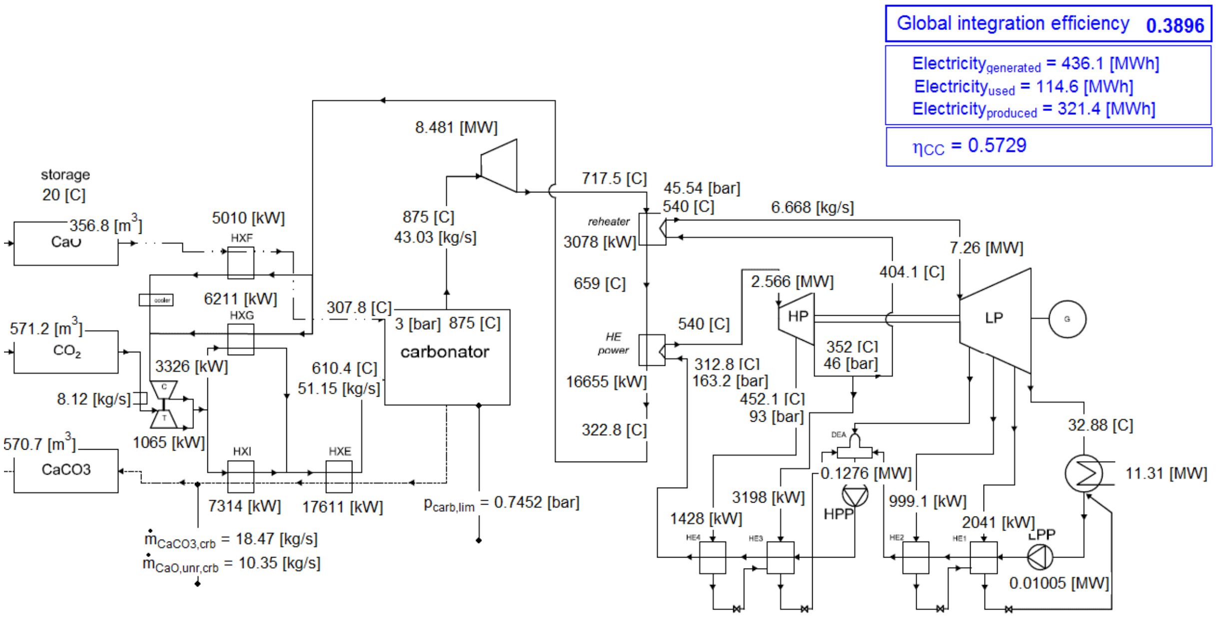

Figure 17: CSP-CaL- CC integration scheme and main simulation results

Figure 18 shows the global cycle performance as a function of the carbonator pressure (or, equivalently, the inlet turbine pressure) for different values of the turbine outlet pressure. As can be seen, a higher performance is obtained by decreasing the outlet turbine pressure, reaching a maximum value of 40.4% for operation under an inlet/outlet turbine pressure ratio of 3.6/1. In order to simplify the heat exchanger network, an atmospheric outlet turbine pressure will be next considered.

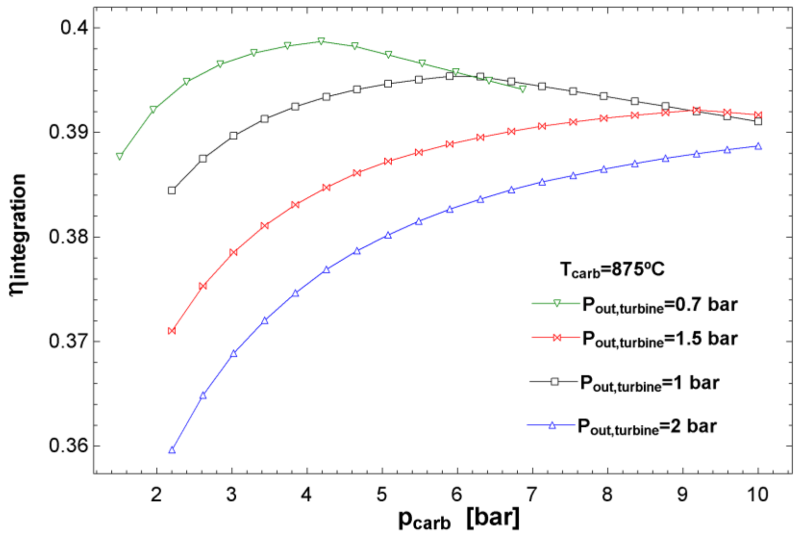

Figure 18: Efficiency of the CSP-CaL-CC integration as a function of the carbonator pressure for several values of the Brayton turbine outlet pressure.

4. Comparative analysis on the CaL-CSP-power cycle integrations

In order to compare the performances of the diverse CSP-CaL-power cycle integrations a sensitivity analysis has been carried out using reference parameters for which the efficiency of these integrations is optimized. Main power cycle parameters for each integration scheme are given in Table 7. A carbonator temperature of 875ºC has been selected, which guarantees carbonation under the different carbonator pressures of each cycle. Unless otherwise indicated, the values of the parameters employed for the CaL cycle are those previously specified in Table 1. Note that temperatures for steam turbine in the case of the combined cycle are conditioned by the Brayton turbine exit and therefore the values shown in this table correspond to the maximum temperatures achievable.

Table 7: Main power cycle parameters for each integration scheme

	Closed CO_2 Brayton	Reheat Rankine	sCO_2 Recompression	Combined cycle
$P_{out,turb}\ (bar)$	1	-	-	1
$P_{carb}\ (bar)$	3.2	1	1	3.2
$P_{vv}\ (bar)$	-	160	-	160
$T_{carb}\ (ºC)$	875	875	875	875
$T_{vv}\ (ºC)$	-	540	-	540
$T_{reheat}\ (ºC)$	-	540	-	540
ΔT_{min}	-	10	10	10
$P[05](bar)$	-	-	75	-
$T[05](ºC)$	-	-	32	-
PR	3.2	-	3	3.2
X	0.5	0.5	0.5	0.5

Figure 19 shows the global integration efficiency obtained for the different power cycles analysed in this work as a function of the carbonator pressure. As can be seen, the CO_2 closed cycle direct integration yields the best efficiency results. Only by means of the indirect integration is possible to operate the carbonator under atmospheric pressure, being the efficiency hampered in this integration as the carbonator pressure is increased further. The opposite trend occurs in the CO_2 closed and CC power cycles. Using these power cycles, the global efficiency is promoted as the carbonator pressure is increased up to a certain optimum value, which is around 4.2 bar for the CO_2 closed cycle and 5.1 bar for the CC cycle (atmospheric turbine outlet pressure). Results show also that despite sCO_2 recompression cycle could be a potentially attractive choice from a thermodynamic point of view, the conservative values used for the turbomachinery efficiencies (in accordance with the current state of art [45,47]) prevents the CSP-CaL-sCO_2 cycle integration from reaching very high global efficiencies. Efficiency results are plotted in Figure 20 as a function of the CaO average conversion. Generally, the enhancement of CaO conversion promotes efficiency as would be expected.

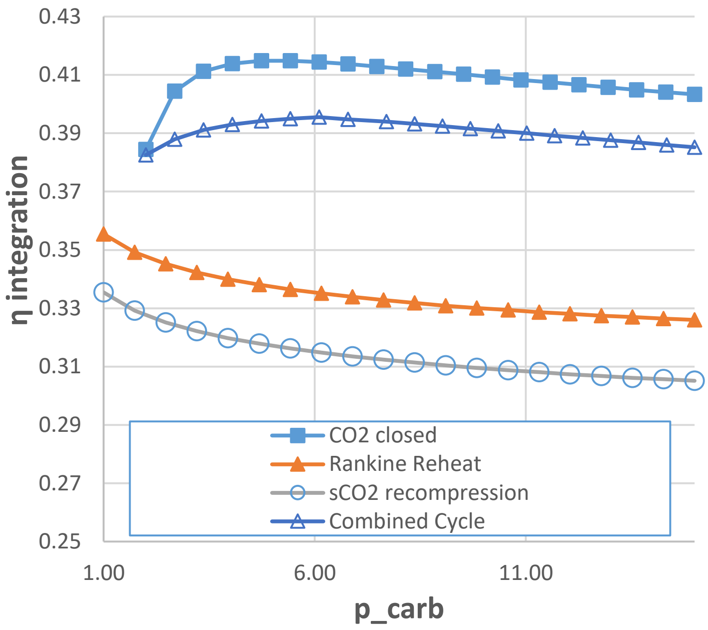

Figure 19: Global cycle integration efficiency as a function of carbonator pressure for the different power cycles coupled to the CSP-CaL system (using data showed in Table 7).

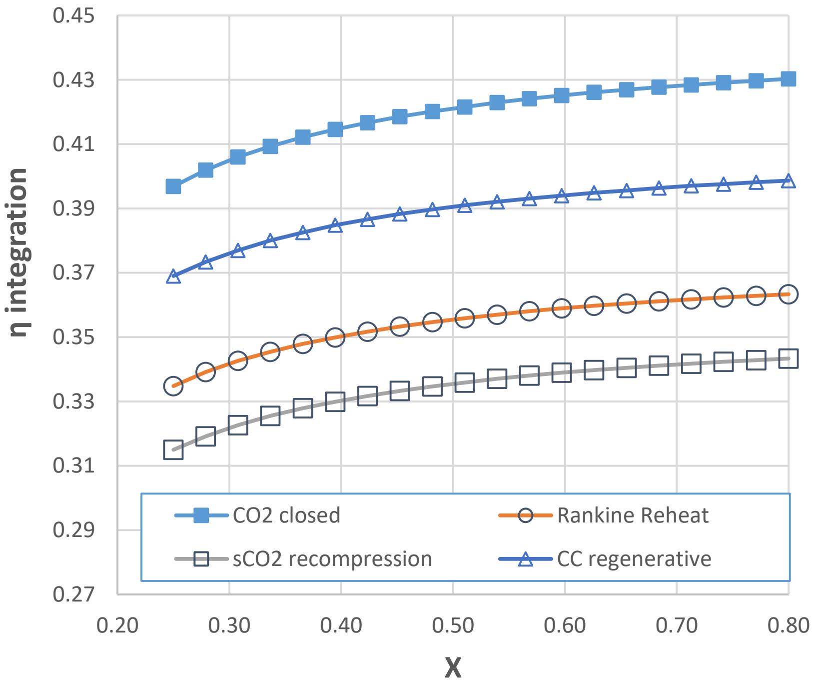

Figure 20: Global cycle integration efficiency as a function of average CaO conversion for the different power cycles coupled to the CSP-CaL system (using data showed in Table 7).

Additional considerations regarding costs must be addressed to further assess the applicability of these power cycle integrations in the CSP-CaL. As this technology is in an early concept stage, data from prototypes or experimental installations are not available for the TCES core.

A detailed economic prospective analysis is under development and will be presented in next works. However, some preliminary considerations can be already made by extrapolating components information from other technologies. In commercial CSP plants, the power block cost percentage is estimated around 32% [63] and power cycle integration has a critical influence on capital investment. Some considerations may be made also on the maturity of the power technologies analysed in this work. These include one full mature technology (steam power cycle), two fully feasible power technologies with already available commercial components (real gas CO_2 closed cycle and the derived combined cycle) and a promising power technology with great advances expected (supercritical CO_2 cycle).

Steam power cycles fulfilling specific conditions for their integration in CSP plants (optimized for complex and challenging cycle conditions) are at the commercial level [64]. For conventional steam power cycles, capital and O&M costs can be estimated as 1280 $/kW and 5.7 $/MWh, respectively [65]. For the CO_2 closed-cycle gas turbine, although not fully available, main components are already usable or can be integrated from different applications. Thermal turbomachinery, compressors and turbines are already in use at commercial scale using as working fluid air, e.g. the Gelsenkirchen plant [66] and Oberhausen I [67], or Helium, e.g. Oberhausen II [67]. In the case of CO_2 as working fluid, compressors are being widely analysed and tested in recent years as fundamental equipment within the Carbon Capture and Storage (CCS) technology [68,69]. Thermal machinery characteristics for the pressure ratios and temperatures presented in this work will be quite similar to the ones operating with air and combustion gases, as shown by Najjar et al. [70] for compressor pressure ratios of 5, compressor temperature inlet of 310 K and turbine temperature inlet of 1100 K. Therefore, already available technologies for turbines and compressors could be employed. In the case of closed-Brayton cycles, the introduction of additional heat exchangers increases capital investment [50]. Therefore, technologies for the conditions presented in this work are already available, and costs for the fully developed technology could be expected as similar to the ones in the range between current gas turbines and combined cycles. For a 100 MWe power block estimated capital and total O&M costs for an open gas turbine combined cycle (considering only the power block) are around 660 $/kW and 2.2 $/MWh, respectively [65,71] whereas for an air-open Brayton cycle they can be estimated as 1026 $/kW and 3.42 $/MWh respectively [72]. Finally, in the case of supercritical CO_2 technology, in spite of that sCO_2 cycle is a non-mature technology, in a project under development granted by US DOE through the Sunshot initiative [73] a power plant investment cost of 1200 $/kW at the commercial stage is assumed [74,75].

Regarding the CaL thermochemical energy storage system, it implies an intrinsic benefit regarding life cycle cost and system sustainability as it is based on the use of low price, non-toxic and widely available natural CaO precursors such as limestone and dolomite. According to [76], the use of the CaL process for TCES would make it possible to achieve a thermal storage cost lower than 15$/kWh$_t$. This preliminary approach shows the potential of these integrations. Detailed and fully developed life cycle and economic analysis are under development and will be the subject of future works.

5. Conclusions

This manuscript analyses several CSP tower plant integration schemes with thermochemical energy storage (TCES) using the Calcium-Looping (CaL) cycle. The work is focused on assessing the power production cycle. The CSP-CaL integration yields high temperatures (above 850ºC) at the power cycle inlet, which allows using high efficiency power cycles employed in fuel based power plants (or combined CSP-fuel power plants). Thus, the CSP-CaL integration achieves high density/long term storage capacity and lends itself for the integration of higher performance power cycles as compared with the current state of the art in commercial CSP plants.

In regards to direct-indirect cycles integration, results show that higher performance is achieved for direct integration. On the other hand, higher efficiencies are attained as the average CaO conversion is increased. Among the power cycles analysed in the present work, the CO_2 closed Brayton cycle shows the best overall performance, reaching efficiencies potentially above 44-45% (including penalty for solids conveying) if the carbonator is operated at temperatures around 950ºC and under pressures about 3.5 bar for atmospheric pressure at Brayton turbine outlet. Importantly, carbonation conditions in this integration allows for high values of the residual conversion of CaO derived from natural minerals such as limestone and dolomite as recently demonstrated by thermogravimetric studies. The wide availability, abundance, lack of corrosiveness, non-toxicity and cheapness (~10$/ton) of these natural minerals makes the proposed integration an attractive technology for large-scale storage of solar energy and highly efficient grid-level power production.

Notation

$c_{p,i}$	Specific heat, kJ/(kmol·K)	$P_{out,turb}$	outlet turbine pressure, bar
$dT\_\min\_HE$	Minimum temperature approach, ºC	y_{eq}	equilibrium fraction of CO_2 in the carbonator
F_i	molar flow rate of component i, kmol/s	T	Temperature, K
F_{CaCO_3}	molar flow rate of $CaCO_3$	T_{carb}	Carbonator temperature, K
$F_{CaCO3,carb}$	molar flow rate of $CaCO_3$ (carbonator side)	$T_{in,CO2}$	CO_2 temperature at carbonator inlet, ºC
$F_{CaCO3,clc}$	molar flow rate of $CaCO_3$ (calciner side)	$T_{in,CaO}$	CaO temperature at carbonator inlet, ºC
$F_{CaO,crb}$	molar flow rate of CaO (carbonator side)	T_{reheat}	Reheat temperature (Rankine cycle), ºC
$F_{CaO,clc}$	molar flow rate of regenerated sorbent	T_{vv}	Live steam temperature, ºC
$F_{CaO,unr,carb}$	molar flow rate of unreacted CaO (carbonator side)	$W_{comp,1}$	compressor 1 power, sCO_2, MW
$F_{CaO,unr,clc}$	molar flow rate of unreacted CaO (calciner side)	$W_{comp,2}$	compressor 2 power, sCO_2, MW
$F_{CO_2,clc,out}$	molar flow rate of CO_2 at calciner outlet	W_{turb}	turbine power, sCO_2, MW
		$\dot{W}$	mechanical power, kW
$F_{R,carb}$	recirculating molar flow rate (carbonator side)	X	CaO conversion X
$F_{R,clc}$	recirculating molar flow rate (calciner side)	X_{slp}	Split factor, sCO_2
h_i	Enthalpy, kJ/kmol	η_c	isentropic compressor efficiency
HXA	solid-solid heat exchanger	η_t	isentropic turbine efficiency
HXB	gas-solid heat exchanger	$\eta_{integration}$	Global integration performance
HXE	gas-solid heat exchanger	$\eta_{storage}$	storage performance
HXF	gas-solid heat exchanger	η_{cycle}	power cycle performance
HXI	gas-solid heat exchanger	η_{cc}	Combined cycle performance
HXG	gas-solid heat exchanger	ϕ_{cycle}	power cycle practicability
$\dot{m}_{CO2,crb}$	CO_2 mass flow rate through carbonator	Δt_{sun}	average daytime period
$\dot{m}_{solids}$	solids mass flow rate, kg/s	$\Delta H_R(T_{react})$	heat of reaction at the reactor temperature
P_{carb}	absolute carbonator pressure, bar	ξ	extent of reaction per unit time

Q_{input}	thermal power input, MW	Φ	heat flux
P_{eq}	CO_2 partial pressure at equilibrium, bar	$\Phi_{carbonation}$	available heat of carbonation
PR	pressure ratio	ε_{rec}	recuperator efficiency, %
p_{drop}	pressure drops in CO_2 circuit, bar	$\Delta P_{R,hot}$	pressure drop recuperator- hot side, %
P_{vv}	Live steam pressure, bar	$\Delta P_{R,cold}$	pressure drop recuperator- coldside, %
$y_{CO2,carb,in}$	inlet molar fraction of CO_2 in the carbonator	$\Delta P_{R,HE}$	pressure drop heat exchanger- sCO_2, %

Acknowledgments

This work was supported by the Spanish Government Agency Ministerio de Economia y Competitividad and FEDER Funds (contracts CTQ2014-52763-C2-1-R, CTQ2014- 52763-C2-2-R and MAT2013-41233-R).

References

[1] United Nations, United Nations. Framework Convention on Climate Change. Adoption of the Paris Agreement. vol. 21932. 2015.
[2] International Energy Agency. Technology Roadmap Solar Thermal Electricity 2014:52. doi:10.1007/SpringerReference_7300.
[3] Kuravi S, Trahan J, Goswami DY, Rahman MM, Stefanakos EK. Thermal energy storage technologies and systems for concentrating solar power plants. Prog Energy Combust Sci 2013;39:285–319. doi:10.1016/j.pecs.2013.02.001.
[4] Mahlia TMIMI, Saktisahdan TJJ, Jannifar A, Hasan MHH, Matseelar HSCSC. A review of available methods and development on energy storage; Technology update. Renew Sustain Energy Rev 2014;33:532–45. doi:10.1016/j.rser.2014.01.068.
[5] Medrano M, Gil A, Martorell I, Potau X, Cabeza LF. State of the art on high-temperature thermal energy storage for power generation. Part 2-Case studies. Renew Sustain Energy Rev 2010;14:56–72. doi:10.1016/j.rser.2009.07.036.
[6] Kearney D, Kelly B, Herrmann U, Cable R, Pacheco J, Mahoney R, et al. Engineering aspects of a molten salt heat transfer fluid in a trough solar field. Energy 2004;29:861–70. doi:10.1016/S0360-5442(03)00191-9.
[7] Fernández AG, Ushak S, Galleguillos H, Pérez FJ. Development of new molten salts with LiNO3 and Ca(NO3)2 for energy storage in CSP plants. Appl Energy 2014;119:131–40. doi:10.1016/j.apenergy.2013.12.061.
[8] Zalba B, Marín JM, Cabeza LF, Mehling H. Review on thermal energy storage with phase change: materials, heat transfer analysis and applications. vol. 23. 2003. doi:10.1016/S1359-4311(02)00192-8.
[9] Pardo P, Deydier a., Anxionnaz-Minvielle Z, Rougé S, Cabassud M, Cognet P. A review on high temperature thermochemical heat energy storage. Renew Sustain Energy Rev 2014;32:591–610. doi:10.1016/j.rser.2013.12.014.
[10] Cot-Gores J, Castell A, Cabeza LF. Thermochemical energy storage and conversion: A-state-of-the-art review of the experimental research under practical conditions. Renew Sustain Energy Rev 2012;16:5207–24. doi:10.1016/j.rser.2012.04.007.
[11] Neveu P, Tescari S, Aussel D, Mazet N. Combined constructal and exergy optimization of thermochemical reactors for high temperature heat storage. Energy Convers Manag 2013;71:186–98. doi:10.1016/j.enconman.2013.03.035.

[12] Janz GJ, Allen, Carolyn B, Bansal NP, Murphy RM, Tomkins RP. Physical Properties Data Compilations Relevant to Energy Storage. II. Molten Salts: Data on Single and Multi-Components Salt Systems. Natl Bur Stand 1979.

[13] N'Tsoukpoe KE, Liu H, Le Pierrès N, Luo L. A review on long-term sorption solar energy storage. Renew Sustain Energy Rev 2009;13:2385–96. doi:10.1016/j.rser.2009.05.008.

[14] Abedin A, Rosen M. A Critical Review of Thermochemical Energy Storage Systems. Open Renew Energy J n.d.:42–6. doi:10.2174/1876387101004010042.

[15] Sakellariou KG, Karagiannakis G, Criado YA, Konstandopoulos AG. Calcium oxide based materials for thermochemical heat storage in concentrated solar power plants. Sol Energy 2015;122:215–30. doi:10.1016/j.solener.2015.08.011.

[16] Rodriguez N, Alonso M, Grasa G, Abanades JC. Heat requirements in a calciner of CaCO3 integrated in a CO2 capture system using CaO. Chem Eng J 2008;138:148–54. doi:10.1016/j.cej.2007.06.005.

[17] Valverde JM, Medina S. Reduction of Calcination Temperature in the Calcium Looping Process for CO_2 Capture by Using Helium: In Situ XRD Analysis. ACS Sustain Chem Eng 2016:acssuschemeng.6b01966. doi:10.1021/acssuschemeng.6b01966.

[18] Romeo LM, Lara Y, Lisbona P, Martínez A. Economical assessment of competitive enhanced limestones for CO2 capture cycles in power plants. Fuel Process Technol 2009;90:803–11. doi:10.1016/j.fuproc.2009.03.014.

[19] Perejon A, Romeo LM, Lara Y, Lisbona P, Valverde JM. The Calcium-Looping technology for CO2 capture: On the important roles of energy integration and sorbent behavior. Appl Energy 2015;162:787–807. doi:10.1016/j.apenergy.2015.10.121.

[20] Sanchez-Jimenez PE, Valverde JM, Perez-Maqueda L. Multicyclic conversion of limestone at Ca-looping conditions: The role of solid-sate diffusion controlled carbonation. Fuel 2014;127:131–40. doi:10.1016/j.fuel.2013.09.064.

[21] Sarrion B, Valverde JM, Perejon A, Perez-maqueda LA, Sanchez-jimenez PE. On the multicycle activity of natural limestone/dolomite for cheap, efficient and non-toxic Thermochemical Energy Storage of Concentrated Solar Power. Energy Technol 2016. doi:10.1002/ente.201600068.

[22] Berger EE. Effect of Steam on the Decomposition of Limestone. Ind Eng Chem 1927;19:594–6. doi:10.1021/ie50209a026.

[23] Frangini S, Masi A. Molten carbonates for advanced and sustainable energy applications: Part I. Revisiting molten carbonate properties from a sustainable viewpoint. Int J Hydrogen Energy 2016;41:18739–46. doi:10.1016/j.ijhydene.2015.12.073.

[24] Fletcher EA, Moen RL. Hydrogen and oxygen from water. Science (80-) 1977;197:1050–6.

[25] Zhang HL, Baeyens J, Degrève J, Cacères G. Concentrated solar power plants: Review and design methodology. Renew Sustain Energy Rev 2013;22:466–81. doi:10.1016/j.rser.2013.01.032.

[26] Siva Reddy V, Kaushik SC, Ranjan KR, Tyagi SK. State-of-the-art of solar thermal power plants - A review. Renew Sustain Energy Rev 2013;27:258–73. doi:10.1016/j.rser.2013.06.037.

[27] Yogi Goswami D. Solar Thermal Power Technology: Present Status and Ideas for the Future. Energy Sources 1998;20:137–45. doi:10.1080/00908319808970052.

[28] Liu M, Steven Tay NH, Bell S, Belusko M, Jacob R, Will G, et al. Review on concentrating solar power plants and new developments in high temperature thermal energy storage technologies. Renew Sustain Energy Rev 2016;53:1411–32. doi:10.1016/j.rser.2015.09.026.

[29] European Academies Scientific Advisory Council. Concentrating solar power: its

potential contribution to a sustainable energy future. 2011.

[30] Tregambi C, Montagnaro F, Salatino P, Solimene R. A model of integrated calcium looping for CO2 capture and concentrated solar power. Sol Energy 2015;120:208–20. doi:10.1016/j.solener.2015.07.017.

[31] Edwards SEB, Materić V. Calcium looping in solar power generation plants. Sol Energy 2012;86:2494–503. doi:10.1016/j.solener.2012.05.019.

[32] Chacartegui R, Alovisio A, Ortiz C, Valverde JM, Verda V, Becerra JA. Thermochemical energy storage of concentrated solar power by integration of the calcium looping process and a CO2 power cycle. Appl Energy 2015. doi:10.1016/j.apenergy.2016.04.053.

[33] Alovisio A, Chacartegui R, Ortiz C, Valverde JM, Verda V. Optimizing the CSP-calcium looping integration for thermochemical energy storage. Energy Convers Manag 2017;In press. doi:10.1016/j.enconman.2016.12.093.

[34] Fidaros DK, Baxevanou C a., Vlachos NS. A parametric study of a solar calcinator using computational fluid dynamics. Energy Convers Manag 2007;48:2784–91. doi:10.1016/j.enconman.2007.07.025.

[35] Meier A, Bonaldi E, Cella GM, Lipinski W, Wuillemin D. Solar chemical reactor technology for industrial production of lime. Sol Energy 2006;80:1355–62. doi:10.1016/j.solener.2005.05.017.

[36] Vignarooban K, Xu X, Arvay A, Hsu K, Kannan AM. Heat transfer fluids for concentrating solar power systems – A review. Appl Energy 2015;146:383–96. doi:10.1016/j.apenergy.2015.01.125.

[37] Mills D. Pneumatic conveying design guide 2004:80.

[38] Barin I. Thermochemical data of pure substances VCH, Weinheim (1989) 1989.

[39] Hanak DP, Anthony EJ, Manovic V. A review of developments in pilot-plant testing and modelling of calcium looping process for CO2 capture from power generation systems. Energy Environ Sci 2015;8:2199–249. doi:10.1039/C5EE01228G.

[40] Grasa GS, Abanades JC. CO2 Capture Capacity of CaO in Long Series of Carbonation/Calcination Cycles. Ind Eng Chem Res 2006;45:8846–51. doi:10.1021/ie0606946.

[41] Romano MC. Modeling the carbonator of a Ca-looping process for CO2 capture from power plant flue gas. Chem Eng Sci 2012;69:257–69. doi:10.1016/j.ces.2011.10.041.

[42] Ortiz C, Chacartegui R, Valverde JM, Becerra JA. A new integration model of the calcium looping technology into coal fired power plants for CO2 capture. Appl Energy 2016;169:408–20. doi:10.1016/j.apenergy.2016.02.050.

[43] Diego ME, Arias B, Grasa G, Abanades JC. Design of a novel fluidized bed reactor to enhance sorbent performance in CO2 capture systems using CaO. Ind Eng Chem Res 2014;53:10059–71. doi:10.1021/ie500630p.

[44] Valverde JM, Sanchez-Jimenez PE, Perez-Maqueda L. Ca-looping for postcombustion CO2 capture: A comparative analysis on the performances of dolomite and limestone. Appl Energy 2015;138:202–15. doi:10.1016/j.apenergy.2014.10.087.

[45] Sánchez D, Muñoz de Escalona JM, Chacartegui R, Muñoz A, Sánchez T. A comparison between molten carbonate fuel cells based hybrid systems using air and supercritical carbon dioxide Brayton cycles with state of the art technology. J Power Sources 2011;196:4347–54. doi:10.1016/j.jpowsour.2010.09.091.

[46] Sánchez D, Chacartegui R, Muñoz De Escalona JM, Muñoz A, Sánchez T. Performance analysis of a MCFC & supercritical carbon dioxide hybrid cycle under part load operation. Int J Hydrogen Energy 2011;36:10327–36. doi:10.1016/j.ijhydene.2010.09.072.

[47] Cheang VT, Hedderwick R a., McGregor C. Benchmarking supercritical carbon dioxide

cycles against steam Rankine cycles for Concentrated Solar Power. Sol Energy 2015;113:199–211. doi:10.1016/j.solener.2014.12.016.

[48] Feher EG. The supercritical thermodynamic power cycle. Energy Convers 1968;8:85–90. doi:10.1016/0013-7480(68)90105-8.

[49] Ahn Y, Bae SJ, Kim M, Cho SK, Baik S, Lee JI, et al. Review of supercritical CO2 power cycle technology and current status of research and development. Nucl Eng Technol 2015;47:647–61. doi:10.1016/j.net.2015.06.009.

[50] Chacartegui R, Muñoz De Escalona JM, Sánchez D, Monje B, Sánchez T. Alternative cycles based on carbon dioxide for central receiver solar power plants. Appl Therm Eng 2011;31:872–9. doi:10.1016/j.applthermaleng.2010.11.008.

[51] Iverson BD, Conboy TM, Pasch JJ, Kruizenga AM. Supercritical CO2 Brayton cycles for solar-thermal energy. Appl Energy 2013;111:957–70. doi:10.1016/j.apenergy.2013.06.020.

[52] Ma Z, Turchi CS. Advanced Supercritical Carbon Dioxide Power Cycle Configurations for Use in Concentrating Solar Power Systems. Supercrit CO 2 Power Cycle Symp 2011:1–4. doi:10.1115/GT2012-68932.

[53] Wright SA, Conboy TM, Rochau GE. High-Temperature Split-Flow Recompression Brayton Cycle Initial Test Results. Nucl Energy 2012.

[54] Moisseytsev A, Sienicki JJ. Investigation of alternative layouts for the supercritical carbon dioxide Brayton cycle for a sodium-cooled fast reactor. Nucl Eng Des 2009;239:1362–71. doi:10.1016/j.nucengdes.2009.03.017.

[55] Sabouhi H, Abbaspour A, Fotuhi-Firuzabad M, Dehghanian P. Reliability modeling and availability analysis of combined cycle power plants. Int J Electr Power Energy Syst 2016;79:108–19. doi:10.1016/j.ijepes.2016.01.007.

[56] Kelly Bruce, Ulf Herrmann MJH. ASME Forum 2001 Integrated Solar Combined Cycle System. Asme 2001.

[57] Alqahtani BJ, Patiño-Echeverri D. Integrated Solar Combined Cycle Power Plants: Paving the way for thermal solar. Appl Energy 2016;169:927–36. doi:10.1016/j.apenergy.2016.02.083.

[58] Okoroigwe E, Madhlopa A. An integrated combined cycle system driven by a solar tower: A review. Renew Sustain Energy Rev 2016;57:337–50. doi:10.1016/j.rser.2015.12.092.

[59] Li Y, Zhou L, Xu G, Fang Y, Zhao S, Yang Y. Thermodynamic analysis and optimization of a double reheat system in an ultra-supercritical power plant. Energy 2014;74:202–14. doi:10.1016/j.energy.2014.05.057.

[60] Manente G. High performance integrated solar combined cycles with minimum modifications to the combined cycle power plant design. Energy Convers Manag 2016;111:186–97. doi:10.1016/j.enconman.2015.12.079.

[61] Li Y, Yang Y. Thermodynamic analysis of a novel integrated solar combined cycle. Appl Energy 2014;122:133–42. doi:10.1016/j.apenergy.2014.02.017.

[62] Zare V, Hasanzadeh M. Energy and exergy analysis of a closed Brayton cycle-based combined cycle for solar power tower plants. Energy Convers Manag 2016;128:227–37. doi:10.1016/j.enconman.2016.09.080.

[63] Zarza E, Romero-Alvarez M. Concentrating Solar Thermal Power. Handb. Energy Effic. Renew. Energy, CRC Press; 2007, p. 21–98. doi:doi:10.1201/9781420003482.ch21.

[64] Siemens. Steam turbines for CSP plants. Siemens AG - Rep 2010:1–16.

[65] Rubin ES, Yeh S, Antes M, Berkenpas M, Davison J. Use of experience curves to estimate the future cost of power plants with CO2 capture. Int J Greenh Gas Control 2007;1:188–97. doi:10.1016/S1750-5836(07)00016-3.

[66] BAMMERT K, BOHNENKAMP W, REHWINKEL H. Results of acceptance tests on

the blast furnace gas and oil fired Gelsenkirchen gas turbine. Stahl Und Eisen 1971;91.

[67] Bentivoglio F, Tauveron N, Geffraye G, Gentner H. Validation of the CATHARE2 code against experimental data from Brayton-cycle plants. Nucl Eng Des 2008;238:3145–59. doi:10.1016/j.nucengdes.2007.12.026.

[68] Tan Y, Nookuea W, Li H, Thorin E, Yan J. Property impacts on Carbon Capture and Storage (CCS) processes: A review. Energy Convers Manag 2016;118:204–22. doi:10.1016/j.enconman.2016.03.079.

[69] Martynov SB, Daud NK, Mahgerefteh H, Brown S, Porter RTJ. Impact of stream impurities on compressor power requirements for CO2 pipeline transportation. Int J Greenh Gas Control 2016;54:652–61. doi:10.1016/j.ijggc.2016.08.010.

[70] Najjar YSH, Zaamout MS. Comparative performance of closed cycle gas turbine engine with heat recovery using different gases. Heat Recover Syst CHP 1992;12:489–95. doi:10.1016/0890-4332(92)90017-C.

[71] NETL. Cost and Performance Baseline for Fossil Energy Plants Volume 1 : Bituminous Coal and Natural Gas to Electricity. vol. 1. 2013.

[72] U.S. Energy Information Administration. Cost and Performance Characteristics of New Generating Technologies , Annual Energy Outlook 2016. 2016.

[73] U.S. Departement of Energy. 2014 SunShot Initiative Portfolio 2014:232.

[74] Moore J. Development of a High Efficiency Hot Gas Turbo-Expander and Low Cost Heat Exchangers for Optimized CSP SCO2 Operation. 2016.

[75] Mehos MS. Beyond LCOE: The Value of CSP with Thermal Energy Storage. Sunshot Program Summit 2016. U.S. Department of Energy. 2016.

[76] Gangwal S, Muto A. Demonstration of High-Temperature Calcium-Based Thermochemical Energy Storage System for Use with Concentrating Solar Power Facilities. Sunshot Program Summit 2016. U.S. Department of Energy. 2016.